International Journal of Bioassays
ISSN: 2278-778X
www.ijbio.com

Research Article

3D QSAR AND PHARMACOPHORE IDENTIFICATION OF ISOQUINOLINE AND BENZIMIDAZOLE ANALOGS AS POTENT C-RAF INHIBITORS

Blessy Christina N[1]*, Manoj Kumar Mahto[2] and Uday Kumar Dasari[1]
[1]Department of human genetics, Andhra University, Visakhapatnam, Andhrapradesh, India
[2]Department of Biotechnology, Nagarjuna University, Guntur, Andhrapradesh, India

Received for publication: August 11, 2013; **Accepted**: September 15, 2013

Abstract: The C-Raf inhibitors obstruct the activity of other signaling pathways which are implicated in many tumors. Hence C-RAF inhibition has emerged as a promising therapeutic target for many cancers. A series of 33 novel Isoquinoline and benzimidazole derivatives has been reported as C-RAF inhibitors. A combined study of pharmacophore prediction, atom based 3d QSAR and molecular docking explored the structural insights of these inhibitors. A Five point pharmacophore hypothesis AADHR. 719 yielded a statistically significant 3D QSAR model with PLS factors as r2= 0.93, Q2= 0.51, RMSE=0.177. Docking study also revealed the binding orientations of active ligand 10e at active site amino acid residue (GLU478, GLN610, PHE443) of C-Raf. The results of ligand based pharmacophore hypothesis and atom based 3D QSAR highlighted the important binding features of novel Isoquinoline and Benzimidazole derivaties as potent C-Raf inhibitors.

Keywords: Pharmacophore, 3D QSAR, Isoquinoline, bezimidazole, C-RAF, Docking

INTRODUCTION

RAS-Mitogen Activated Protein Kinase (MAPK) (Zebisch and Troppmair, 2006) pathway plays an integral role in transducing signals from cytokines and growth factors to promote cell adhesion, proliferation, migration and survival through Receptor Tyrosine Kinases (RTK) (Katz M *et al.,* 2007). RAS plays a central role in this signaling cascade, where a small membrane bound GTPase shuttles between active GTP-bound and inactive GDP-bound. It is activated by guanine exchange factor, Son of Sevenless (SOS) usually found in the cytoplasm of the cell (Oliver Dreesen and Ali H. Brivanlou, 2007). Receptor signaling shuttles SOS to the cell membrane to catalyze the nucleotide exchange reaction of RAS. Activated GTP-bound RAS activates the RAF, which in turn activates mitogen-activated protein kinases (MAPK) also known as extracellular signal-regulated kinase (ERK). ERK/MAPK translocates to the nucleus where several transcription factors are activated. Further phosphorylation of MAPK is obstructed by RAF Kinase Inhibitor Protein. Mutations on RAF and RAS are observed in a broad spectrum of human tumors. RAF mutations are found in roughly two thirds of all melanoma (Sebolt-Leopold *et al.,* 2004). Therefore RAS-RAF-MEK-MAPK pathway is considered to be therapeutic intervention in cancer. The three RAF isomers (RAF-1 or C-RAF, A-RAF, B-RAF) will interact with RAS and activate the MAPK pathway, it has also been shown that B-RAF interacts with C-RAF and activates C-RAF in RAS dependent manner. Small molecules of RAF kinase inhibitors containing diverse scaffolds have emerged. Sorafenib is used for the treatment of renal cell carcinoma; its activity against certain tumor types is due to inhibition of other kinases like VEGFR rather than RAF (Ramurthy S *et al.,* 2008). It has been found that structural modifications of Sorafenib have optimized the activity of C-RAF. Sorafenib is an ATP competitive inhibitor (Wilhelm *et al.,* 2008). Modification of Sorafenib leads to two the series of inhibitors (Isoquinoline and Benzimidazole). From both the series it has been found that bicyclic hetrocycles are key elements for interaction with hinge region of C-RAF. Over all it is confirmed that substitution of the phenyl ring with lipophilic substituents are needed for potent RAF inhibition (Tang J *et al.,* 2008)

In present study 32 inhibitors (Isoquinoline and Benzimidazole) were obtained from the literature. In rational drug design approach Pharmacophore Alignment and Scoring Engine (PHASE) software was used to develop ligand-based pharmacophore model development (Talele *et al.,* 1999; Karki and Kulkarni, 2001). Pharmacophore development, 3D quantitative structure activity relationship (3D QSAR) (Juvale *et al.,* 2006; Gokhale *et al.,* 2000; Kharkar *et al.,* 2009) and molecular docking studies were performed to study the functionalities that may influence the activity and to characterize the binding mode between the most active ligand and C-RAF.

MATERIALS AND METHODS

Data set:

33 novel Inhibitors of C-RAF were taken from available literature (Hans-peter Buchstaller *et al.,* 2011) are given in Table 1 and Table 2 with their biological activities in terms of IC_{50} values. The 33 compounds

***Corresponding Author:**
Blessy Christina N,
Department of human genetics,
Andhra University, Visakhapatnam,
Andhrapradesh, India.

selected had IC_{50} values of different range therefore the values (in moles/litre) were converted into negative logarithm of IC_{50} (pIC_{50}). pIC_{50} above 6.5 were considered as active and below 6.5 were considered as inactive. The data set was divided into active set of 19 molecules and inactive set of 14 molecules.

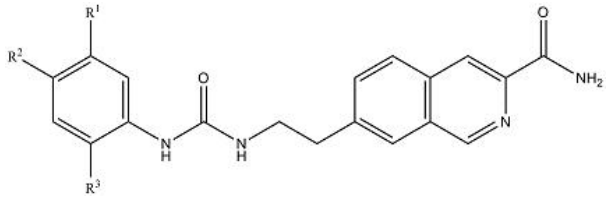

Fig. 1: Structure of isoquinoline

Table.1: C-Raf inhibitors of isoquinoline derivative

Compound	R1	R2	R3	IC50	PIC50 Observed	PIC50 Predicted	Residual	Pharma Set	QSAR Set
10a	CF_3	H	H	0.36	6.444	6.44	0.004	Inactive	Test
10b	OCF_3	H	H	0.26	6.585	6.65	-0.065	Active	Test
10c	SO_2CF_3	H	H	0.20	6.699	6.57	0.129	Active	Test
10d	H	CF_3	H	0.37	6.432	6.42	0.003	Inactive	Training
10e	CF_3	CF_3	H	0.20	6.699	6.74	-0.041	Active	Test
10f	CF_3	Cl	H	0.16	6.796	6.75	0.046	Active	Test
10g	CF_3	F	H	0.24	6.620	6.75	-0.13	Active	Test
10h	CF_3	H	F	0.25	6.602	6.64	-0.038	Active	Training
10i	CF_3	H	OCH_3	0.12	6.921	6.92	0.001	Active	Training
10j	CF_3	H	$O(CH_2)_2N(CH_3)_2$	0.45	6.347	6.69	-0.343	Inactive	Test
10k	Cl	CH_3	OCH_3	0.11	6.959	6.91	0.049	Active	Training
10l	CH_3	Cl	OCH_3	0.19	6.721	6.75	-0.029	Active	Training
10m	CF_3	Cl	OCH_3	0.08	7.097	6.79	0.307	Active	Test
10n	CF_3	Cl	$O(CH_2)_2N(CH_3)_2$	0.34	6.469	6.41	0.059	Inactive	Training

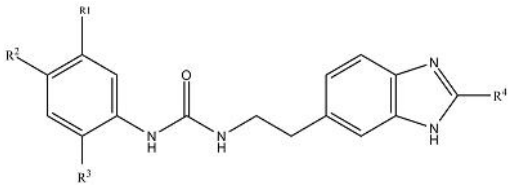

Fig. 2: Structure of benzimidazole

Table.2: C-Raf inhibitors of Benzimidazole derivative

Compound	R1	R2	R3	R4	IC50	PIC50 Observed	PIC50 Predicted	Residual	Pharma Set	QSAR Set
19a	CF_3	H	OCH_3	$CONHCH_3$	0.34	6.469	6.52	-0.051	Inactive	Training
19b	CF_3	H	OCH_3	$NHCOOCH_3$	0.81	6.092	6.13	-0.218	Inactive	Test
19c	CF_3	H	OCH_3	$NHCOCH_3$	0.17	6.770	6.71	0.06	Active	Training
19d	CF_3	Cl	H	$NHCOOCH_3$	0.28	6.553	6.60	-0.047	Active	Training
19e	CF_3	Cl	H	$NHCOCH_3$	0.66	6.180	6.13	0.05	Inactive	Training
19f	CF_3	Cl	H	$NHCOCH_3$	0.14	6.854	6.73	0.124	Active	Training
19g	CF_3	H	H	$NHCOCH_3$	0.48	6.319	6.41	-0.091	Inactive	Training
19h	Cl	Cl	H	$NHCOCH_3$	0.48	6.319	6.38	-0.061	Inactive	Test
19i	Cl	CH_3	H	$NHCOCH_3$	0.53	6.276	6.35	-0.074	Inactive	Training
19j	Cl	CH_3	OCH_3	$NHCOCH_3$	0.19	6.721	6.77	-0.049	Active	Training
19k	CH_3	Cl	OCH_3	$NHCOCH_3$	0.32	6.495	6.68	-0.185	Inactive	Test
19l	CH_3	H	$O(CH_2)_2NHCH_3$	$NHCOCH_3$	0.58	6.237	6.18	0.057	Inactive	Training
19m	CH_3	Cl	$O(CH_2)_2NHCH_3$	$NHCOCH_3$	0.49	6.310	6.33	-0.02	Inactive	Training
19n	CF_3	H	$O(CH_2)_2NHCH_3$	$NHCOCH_3$	0.21	6.678	6.68	-0.002	Active	Training
19o	CF_3	Cl	$O(CH_2)_2NHCH_3$	$NHCOCH_3$	0.23	6.638	6.57	0.068	Active	Training
19p	CH_3	Cl	$O(CH_2)_2NH_2$	$NHCOCH_3$	0.55	6.260	6.52	-0.26	Inactive	Test
19q	CF_3	H	$O(CH_2)_2NH_2$	$NHCOCH_3$	0.25	6.602	6.64	-0.038	Active	Training
19r	CF_3	Cl	$O(CH_2)_2NH_2$	$NHCOCH_3$	0.18	6.745	6.53	0.215	Active	Test
19s	CF_3	H	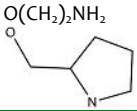	$NHCOCH_3$	0.23	6.638	6.69	-0.052	Active	training

Ligand preparation:

Before the task of pharmacophore model development, low energy 3D structures of all molecules of interest must be available. Accordingly we have minimized the structures by using impact minimization. We also incorporated structure cleaning step, which generates stereoisomers, and, neutralizes charged structures. All the structures were minimized at pH ranges from 5-9 using ligprep. Conformers were generated with force field OPLS- 2005 (Kaminski, 2010; Amnerkar and Bhusari, 2010) and with maximum number of conformers per structure as 1000 (Chang *et al.,* 1989; Kolossvary *et al.,* 1996) with RMSD 1.0 A°.

Hypothesis generation:

PHASE used to identify the functional groups that are common for biological activity of the ligands which are under investigation (Dixon SL *et al.,* 2006a; Evans DA *et al.,* 2007). PHAGE contains a standard set of six pharmacophore feathers hydrogen bond acceptor (A), hydrogen bond donor (D), hydrophobic group (H), negatively ionizable (N), positively ionizable (P), and aromatic ring (R). These set of feature types that define a possible pharmacophore-using a tree-based partitioning algorithm. Common pharmacophore hypothesis (CPH) was identified from the set of variants with the option create sites, maximum and minimum features as 5, total number of matches to 4, others were kept to default, this gives 84 variants. Hypothesis generation was done by using find option which generated hypothesis for 54 variants. Further, CPH was selected depending on the survival score until at least one hypothesis was found and scored successfully. Score was calculated for both actives and inactives using default parameters for vector, site, and volume, number of matches, selectivity, and energy terms.

3D QSAR:

3D QSAR models were generated with the selected pharmacophore hypothesis with best score. In the alignment option, align non-model ligands were chosen to align the ligands that are not part of the active set. In Build QSAR option random training set was kept as 60% which generates training set of 20 molecules and test set of 13 molecules. Atom based model was generated by keeping 1Å grid spacing and 3 as maximum number of Partial least square (PLS) factors. The accuracy of the models increases with increasing number of PLS factors

Molecular docking study:

Docking was performed using glide. C-Raf structure was retrieved from protein data bank (PDB ID: 3OMV). Further protein was preprocessed, optimized and minimized with force field OPLS2005 and RMSD of 0.03A^{O} in protein preparation wizard. Grid is generated using Glide application with residue number PHE475 in chain A. By "enabling write XP descriptor" docking was performed and rest all parameters are kept as default.

RESULTS AND DISCUSSION

Pharmacophore model development:

A total of 54 different variant hypotheses were generated upon completion of common pharmacophore identification process. Those pharmacophore models whose scores ranked in the top were selected (Dixon S L *et al.,* 2006b) The top model was found to be associated with the five point hypotheses which consist of two hydrogen bond acceptors (AA), one hydrogen bond donor (D), one hydrophobic group (H) and one ring (R) features. The best pharmacophore model was resulted from AADHR. 719 whose survival score are 3.747 with PLS factor as 3. This hypothesis showing distance between pharmacophoric sites is depicted in (Fig. 3). Summary generated from AADHR is shown in the Table 3. Plots of predicted vs actual PIC_{50} for training and test set were reported in (Fig. 4).

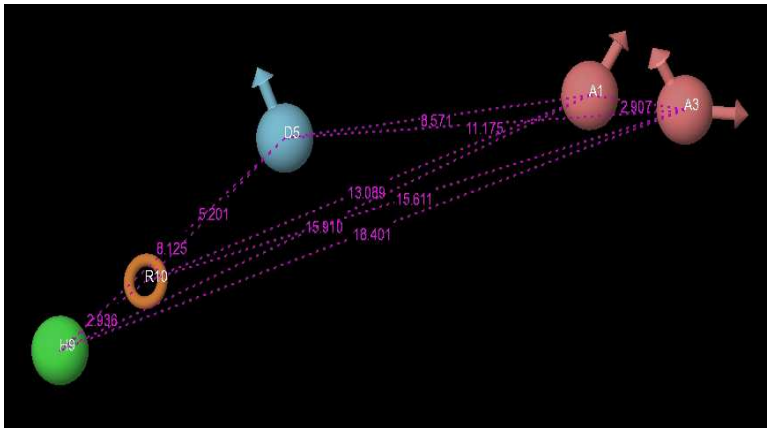

Fig.3: Pharmacophore hypothesis and distance between pharmacophoric sites in Å unit.

Table.3: QSAR results of pharmacophore.

Hypothesis	r2	F	Q2	SD	P	RMSE	Pearson-R
AADHR	0.93	78.2	0.51	0.06	8.937e-010	0.177	0.73

SD = standard deviation of the regression
r2 = correlation coefficient
P = significance level of variance ratio, F = variance ratio
Q2 = for the predicted activities, RMSE = root-mean-square error
Pearson-R = correlation between the predicted and observed activity for the test set

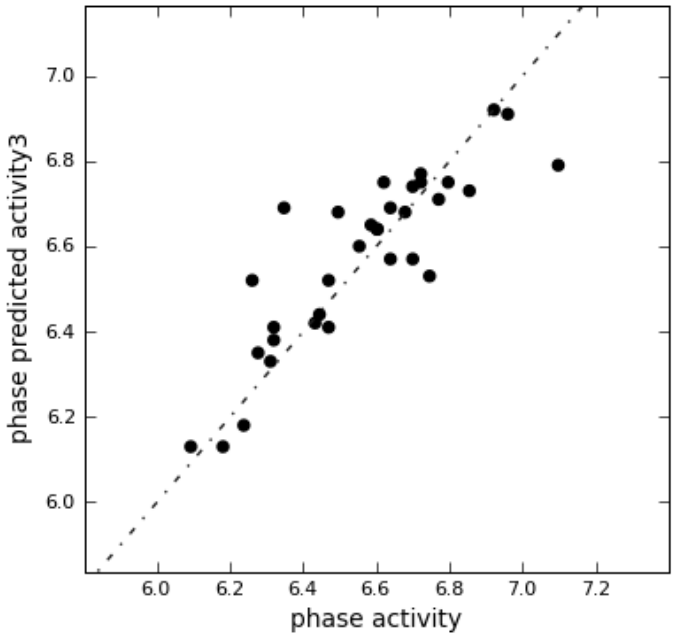

Fig. 4: Graph of actual phase versus predicted pIC50 of the training and test set using atom based QSAR model from PHASE.

Analysis of atom based 3D QSAR model:

The inhibitory activity can be gained by visualizing the QSAR model of most active and least active compounds. The maps obtained from Hypothesis shows how 3D-QSAR methods can identify features important for the interaction between ligands and their target protein. Such maps allow identification of those positions that require a particular property to enhance the bioactivity of a ligand. A pictorial representation of the maps generated is shown in Fig. 5a–f. In these maps, the blue cubes indicate favorable regions while red cubes indicate unfavorable regions for activity.

Fig. 5a and b compares of the most significant favorable and unfavorable electron with drawing features that arise when the QSAR model is applied to the most active compound 10e and least active compound 19n. The blue cubes are observed near isoquinoline derivative, and near 2-carboxy amide group of compound 10e. This suggests that these features are important for the activity of the molecule and these functional groups should not be unsubstituted. Hence isoquinoline moiety increases the activity of compound 10e. In compound 19n few red cubes were observed 2-carboxy amide group, no blue cubes are near benzimidazole group which is not aligned properly and decreases its activity.

Fig. 5c and d compare the most significant favorable and unfavorable hydrogen bond donor that arise when the QSAR model is applied to the most active compound 10e and least active compound 19f. Blue cubes where observed near 2-carboxy amide group and isoquinoline derivative indicating their importance for activity in context to compound 10e, which again clearly shows isoquinoline substitution is important for the activity. A1 and A3 are not properly aligned with the ligand in context to compound 19n.

We also examined the QSAR model of a compound with best hydrophobic property Fig 5e and f. It was observed that more favorable regions are observed in 10e in the region of isoquinoline moiety and lipophilic substituents (R1) of phenyl ring than the substituents of compound 19n.

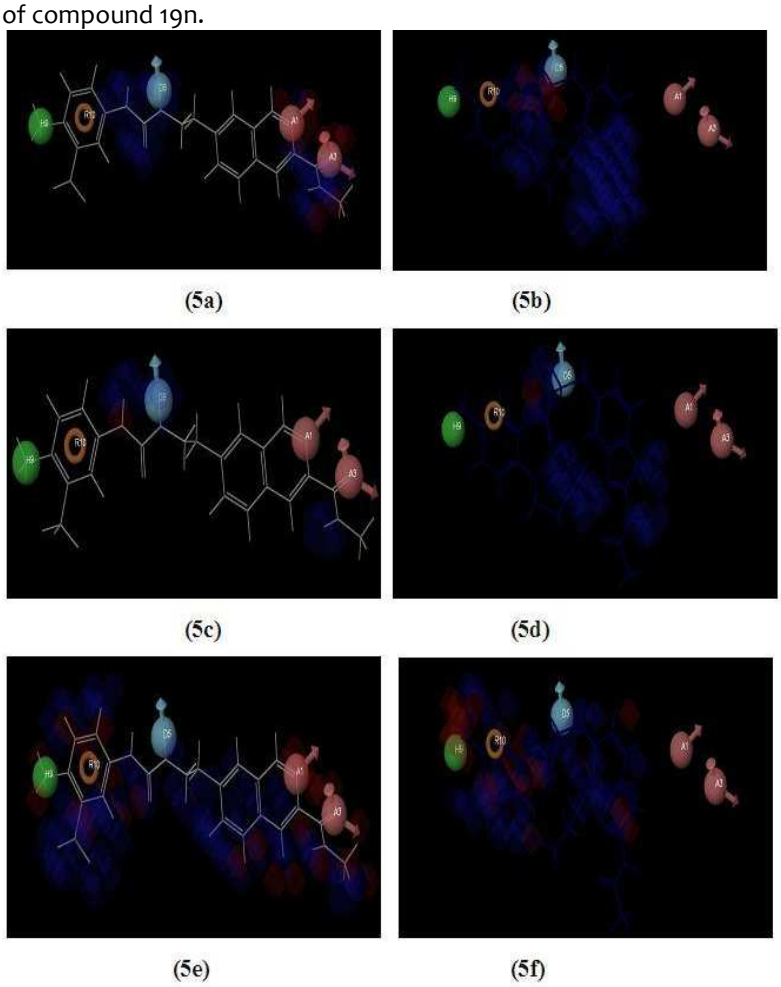

Fig. 5: Pictorial representation of cubes generated using the QSAR. Blue indicate favorable regions and red indicate unfavorable regions, QSAR model visualized the electron withdrawing group of the most active compound 5 (a), least active compound 5 (b) and hydrogen bond donor of the most active compound 5 (c), least active compound 5 (d). QSAR model representing the hydrophobic property of the most active compound 5 (e), least active compound 5 (f)

Docking results:

Detailed intermolecular interaction between ligand and the targeted protein was performed using, automated molecular docking software Glide. Docking study shows the binding mode of the active compound 10e on c-Raf and to obtain information for further

structure optimization (Fig. 6). Docking analysis shows the following interactions. 2- Carboxyamide group interacts with oxygen of amino acid residue GLU478, Phenyl ring of isoquinoline will interacts with Nitrogen atom of GLN610 and amine group of isoquinoline will interacts with oxygen atom of PHE443 which plays crucial role c-raf inhibitory activity.

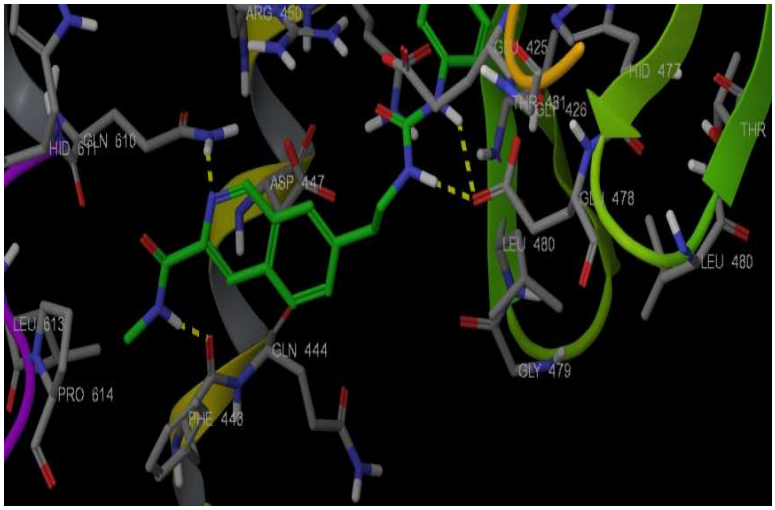

Fig. 6: docking of compound 10e in the active site of c-Raf

CONCLUSION

In conclusion, the highly predictive atom based 3D QSAR model was generated using 33 molecules which consists of five pharamacophore hypothesis AADHR. 719. The development of atom based 3D QSAR has provided the requirement of novel series of Isoquinoline and benzimidazole as potent C-RAF inhibitors. The pharmacophore based study indicated the possible hydrophobic, Electron withdrawing and Hydrogen bond donor interactions of ligand with C-RAF. Docking gives a hypothetical image to design new potent C-RAF inhibitors.

ACKNOWLEDGMENT

We thank Raghu Rangaswamy, Andhra University, Senior Director and Vinod Devaraji, IT consultant from Schrodinger for providing free academic evaluations software and continuous support to undertake this research work.

REFERENCES

1. Amnerkar NA, Bhusari KP (2010) Synthesis, anticonvulsant activity and 3D-QSAR study of some prop-2-eneamido and 1-acetylpyrazolin derivatives of aminobenzothiazole. Eur Med Chem 45:149–159.

2. Chang G, Guida W C, Still w C (1989) An internal-coordinate Monte Carlo method for searching conformational space. J. Am. Chem. Soc 111: 4379-4386.

3. Dixon S L, Smondyrev A M, Knoll E H, Rao S N, Shaw D E, Friesner R. A (2006b) PHASE: a new engine for pharmacophore perception, 3D QSAR model development, and 3D database screening: 1. Methodology and preliminary results. J. Comput. Aided Mol. Des 20: 647–671.

4. Dixon SL, Smondyrev AM, Rao SN (2006a) PHASE: a novel approach to pharmacophore modeling and 3D database searching. Chem Biol Drug Des 67:370–372.

5. Evans DA, Doman TN, Thorner DA, Bodkin MJ (2007) 3D QSAR methods: phase and catalyst compared. J Chem Inf Model 47:1248–1257.

6. Gokhale V M, Kulkarni V M (2000) Understanding the antifungal activity of terbinafine analogues using quantitative structure–activity relationship (QSAR) models. Bioorg. Med.Chem 8: 2487 2499.

7. Hans-peter Buchstaller, Lars Burgdorf, Dirk Finsinger, Frank Stieber, Christian Sirrenberell, Christiane Amendt, Matthians Grell, Frank Zeneke, Mireille Kirer (2011) Design and synthesis of isoquinoline and benzimidazoles as RAF kinase inhibitors. Bioorganic and medicinal chemistry letters 21: 2264-2269.

8. Juvale D C, Kulkarni V V, Deokar H S, Wagh N K, Padhye S B, Kulkarni V M (2006) 3D-QSAR of histone deacetylase inhibitors: hydroxamate analogues. Org. Biomol. Chem 4: 2858-2868.

9. Kaminski GA, Friesner RA, Tirado-Rives J, Jorgensen WL (2001) Evaluation and reparameterization of the OPLS-AA force field for proteins via comparison with accurate quantum chemical calculations on peptides. J Phys Chem B 105: 6474–6487.

10. Karki R. G, Kulkarni V. M (2001) A feature based pharmacophore for Candida albicans MyristoylCoA: protein N-myristoyltransferase inhibitors. Eur. J. Med Chem.36: 147-163

11. Katz M, Amit and Yarden Y (2007) Regulation of MAPKs by growth factors and receptor tyrosine kinases. Biochimica et Biophysica Acta 1773: 1161-76.

12. Kharkar P S, Deodhar M N, Kulkarni V M (2009) Design, synthesis, antifungal activity, and ADME prediction of functional analogues of terbinafine. Med. Chem. Res 18: 421- 432.

13. Kolossvary I, Guida W C (1996) Low mode search An efficient, automated computational method for conformational analysis: application to cyclic and acyclic alkanes and cyclic peptides. J. Am. Chem. Soc 118: 5011-5019.

14. Oliver Dreesen & Ali H. Brivanlou (2007) Signaling Pathways in Cancer and Embryonic Stem Cells. Humana Press IncStem Cell Rev DOI 10.1007/s12015-007-0004-8.

15. Ramurthy S, Subramanian S, Aikawa M et al (2008) Design and synthesis of orally bioavailable benzimidazoles as Raf kinase inhibitors.Med. Chem 27: 7049 52.

16. S.M. Wilhelm, L. Adnane, P. Newell, et al (2008) Preclinical overview of sorafenib, a multikinase inhibitor that targets both Raf and VEGF and PDGF receptor tyrosine kinase signaling. Mol. Cancer Ther 7: 3129–3140.

17. Sebolt-Leopold, J. S, & Herrera R. (2004) Targeting the mitogen-activated protein kinase cascade to treat cancer. Nature Reviews. Cancer 4: 937–947.

18. Talele T, Kulkarni S, Kulkarni V M (1999) Development of pharmacophore alignment models as input for comparative molecular field analysis of a diverse set of azole antifungal agents. J. Chem. Inf. Comput. Sci 39: 958-966.

19. Tang J, Hamajima T, Nakano M, Sato H, Dickerson S H, Lackey K E (2008) Knowledge-based design of 7-azaindoles as selective B-Raf inhibitors. Bioorg. Med. Chem. Lett 18: 4610-4.

20. Zebisch, J. Troppmair (2006) Back to the roots: the remarkable RAF oncogene story. Cell. Mol. Life Sci 63: 1314–1330.

Source of support: Nil
Conflict of interest: None Declared